Polarized Band-Edge Emission and Dichroic Optical Behavior in Thin Multilayer GeS

Ching-Hwa Ho and Jia-Xuan Li*

Because of the enthusiastic study of graphene, quasi-two-dimensional (2D) layered compounds such as transition-metal dichalcogenides (TMDCs) and group III and IV chalcogenides are of sustained interest. This interest is because thin-layer chalcogenides can be obtained by van der Waals exfoliation and they show specific semiconducting, electrical, and opto-electronical properties that are desirable for various device applications in both monolayer and multilayer form.[1–4] For chalcogenides, the direct or indirect band-gap is a crucial factor for application of these 2D materials in optoelectronics and luminescence devices. Many of the TMDCs (such as MoS_2 and WSe_2) are generally indirect semiconductors in their bulk or multilayer form. Research interest in TMDCs is partly because their band-gaps can undergo indirect-to-direct transition when their thickness approaches that of a monolayer.[5] For the III–VI and IV–VI layered compounds, GaSe and InSe in their multilayer form are essentially direct semiconductors with a direct band-gap of ca. 2.0 (GaSe) and 1.24 eV (InSe).[6,7] For a IV–VI GeS layer compound, the theoretical calculation of monolayer GeS reveals that it is an indirect semiconductor ($E_g \approx 2.34$ eV).[8] Nevertheless, multilayer GeS may be a direct semiconductor with a band-gap approaching 1.6 eV.[9] Thin multilayer GeS with a thickness of below 100 nm is suitable for device fabrication but was rarely studied to date. The emission and optical properties of the thin multilayer GeS need further exploration to promote their extensive applications.

GeS crystallizes in a layered structure of orthorhombic symmetry of space group D^{16}_{2h}, which contains eight atoms in an unit cell of lattice constants $a = 4.30$, $b = 3.64$, and $c = 10.47$ Å.[10] Each of the monolayers stack along the c axis and the unit cell comprises two adjacent double layers.[10,11] Layered GeS has received more attention than its monolayer equivalent because of its suitable band-gap (ca. 1.5–1.7 eV)[12,13] and high absorption coefficient for solar-cell fabrication, excellent cycling performance for reversible lithium batteries,[14] anisotropic optical property,[15] as well as for being considered a "green" material and sustainable. Previous research focused mostly on bulk GeS and seldom on the nanoscale. The nanoscale structural and optical absorption behaviors of GeS nanosheets have been studied and proposed for energy applications,[16,17] however, the light-emitting property of a thin multilayer GeS was not yet explored.

Herein, in-plane optical anisotropy of band-edge emission of a multilayer GeS stripe ($t \approx 40$ nm) is characterized by using polarized micro-photoluminescence (μPL) measurement with polarization angles ranging from 0 to 90° with respect to the multilayer's longest crystal edge (b axis). Light emission from multilayer GeS is completely forbidden at $\theta = 0°$ (E||b), and fully allowed (intense light) at $\theta = 90°$ (E||a), which obeys a dichroic Malus law[18] for the emission peak at 1.622 eV. Multilayer GeS behaves like a dichroic light emitter with linear polarization along the multilayer's a axis. To understand the band-edge characteristic of the GeS multilayer, polarized thermoreflectance (PTR) measurement by using microscope white-light guiding was also implemented. The selection rule of the PTR spectra also reveals that the lower band-edge transition $E_A = 1.622$ eV is only allowed with E||a polarization while another higher energy transition, $E_B = 1.732$ eV, appears merely along the E||b polarization in the multilayer. In-plane anisotropy of the c plane GeS multilayer occurs with linear polarization along a and b axes. The energy position of the E_A transition matches well with the main band-edge emission observed by μPL, while the E_B transition may probably originate from valence-band splitting (dominated by the S p orbital) of the multilayer GeS. The structural and optical anisotropy of the multilayer GeS is discussed here.

Layered single crystals of IV–VI GeS with different areas, sizes, and thicknesses were grown by using the chemical vapor transport (CVT) method[19] with iodine as the transport agent. The crystals were prepared from their elements (Ge: 99.999% pure and S: 99.999%) by reaction at 600 °C for two days in evacuated quartz ampoules. Sulfur was added in 1 mol% excess with respect to the stoichiometric mixture of the constituent elements. About 10 g of the elements, together with an appropriate amount of transport agent (I_2 about 10 mg cm^{-3}), were introduced into a quartz ampoule (22 mm OD, 17 mm ID, 20 cm length), which was then cooled with liquid nitrogen, evacuated to 10^{-6} Torr and sealed. The mixture was slowly heated to 600 °C and maintained at this temperature for two days. The temperature was then altered from 600 °C (heating zone) → 520 °C (growth zone) with a gradient of –4 °C cm^{-1} for crystal growth. The reaction was left 240 h to produce large single crystals. The as-grown GeS crystals are dark red and have a shiny surface with an area of up to 5 mm^2 and thickness of up to 100 μm. The crystals are mostly like ribbon or stripe-shape layered crystals (see Figure S1 in the Supporting Information). The powder and single-crystal X-ray diffraction (XRD) results of GeS shown in Figure S1 reveal an orthorhombic phase. The lattice constants are a = 4.36 Å, b = 3.67 Å, and c = 10.53 Å,

Prof. C.-H. Ho, J.-X. Li
Graduate Institute of Applied Science and Technology
National Taiwan University of Science and Technology
Taipei 106, Taiwan
E-mail: chho@mail.ntust.edu.tw
Prof. C.-H. Ho
Graduate Institute of Electro-Optical Engineering and
Department of Electronic and Computer Engineering
National Taiwan University of Science and Technology
Taipei 106, Taiwan

DOI: 10.1002/adom.201600814

as calculated from the XRD patterns. Energy-dispersive X-ray (EDX) analysis indicates that the stoichiometry of Ge:S of the as-grown crystal is about 1:1. The weak van der Waals bonding between the layers means that the GeS crystal can be separated (to about nm) from its layer (*c*) plane by using Scotch tape with mechanical exfoliation. The thin exfoliated GeS nanoflakes were transferred onto a SiO_2/Si substrate about $8 \times 8 \times 0.3$ mm^3.

The μPL and micro-Raman (*μ*Raman) measurements of GeS multilayer were carried out by using a RAMaker integrated *μ*Raman–PL system equipped with a 532-nm solid-state diode-pumped laser and a 633-nm He–Ne laser as the excitation sources. A light-guiding microscope (LGM) equipped with an Olympus objective lens (50×, working distance ca. 8 mm) acted as the interconnection-coupled medium between the nanosheet sample, incident and reflected lights, and charge-coupled-device (CCD) spectrometer. The 633-nm laser was the pumping light source of the μPL measurement. A pair of dichroic sheet polarizers (visible to infrared range) was utilized for polarization-dependent measurements. A Janis liquid-helium open-cycled cryostat facilitated low-temperature measurement of the multilayer GeS. A Lakeshore 335 digital thermometer controller was used for temperature-dependent measurement between low and room temperatures. For TR measurement of the multilayer GeS, a 60-W tungsten halogen lamp acted as the white-light source. The same LGM system as that of μPL was used for guiding the incident and reflected white light. The reflected light of the multilayer GeS sample from LGM was coupled into a PTI 0.2-m monochromator equipped with a 1200 grooves per millimeter grating. The dispersed output light of different photon energy was scanned and detected by using an EG&G HUV2000B Si photodetector. For thermal modulation of the multilayer sample, a gold-evaporated quartz substrate acted as the heating element. The GeS-nanoflake decorated SiO_2/Si substrate was closely attached to the heating element and then mounted onto the low-temperature cryostat holder. Thermal modulation of the sample was achieved by supplying periodic current pulses to the Au heating element.[20] Heat generation and dissipation from the Au tracks and the substrate must be well balanced to avoid any increase of temperature in the sample (i.e., weak heating disturbance). A 4-Hz square wave was employed in the TR experiments. For PTR measurements, a pair of dichroic sheet polarizers was used. The thickness of the multilayer specimen was measured by using atomic force microscopy (AFM).

Figure 1 shows the *c*-plane high-resolution transmission electron microscope (HRTEM) image and selected-area diffraction pattern (SADP) of electrons in the multilayer GeS that was exfoliated from bulk crystal. Clear and regular atomic sites on a large-area HRTEM image, as well as obvious dotted pattern on

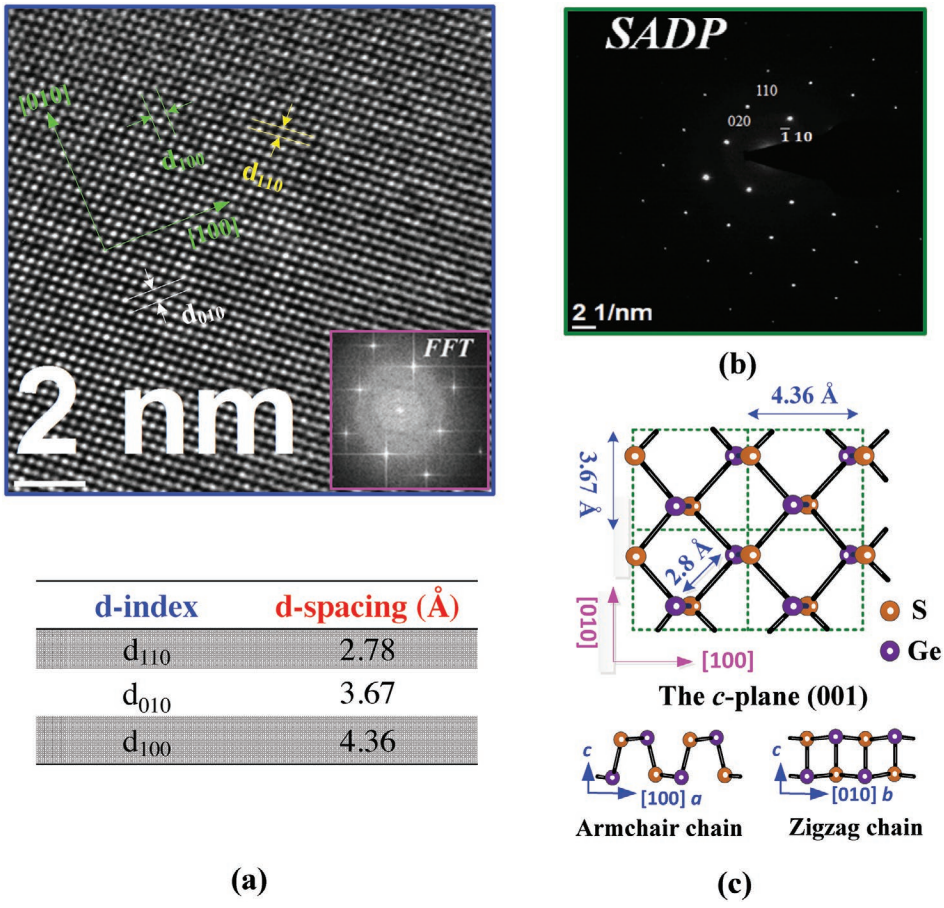

d-index	d-spacing (Å)
d_{110}	2.78
d_{010}	3.67
d_{100}	4.36

Figure 1. a) HRTEM image of the *c*-plane multilayer GeS grown by CVT. The crystal orientations and interplanar spacing related to the *a* and *b* axes are indicated. The inset shows the FFT pattern of the HRTEM result. b) The SAED pattern of the multilayer GeS. c) The representative schemes of the atomic arrangement of GeS viewed along *c* (top), *b* (lower left) and *a* (lower right) axes.

the SADP, indicate that high quality crystallinity of the as-grown GeS multilayer was obtained by CVT. The orientations of *a* and *b* axes ([100] and [010]) are clearly shown in Figure 1a; this demonstrates orthogonality and presents evidence of an orthorhombic crystalline phase. The interplanar spacing of d_{110}, d_{010}, and d_{100} is estimated to be 2.78, 3.67, and 4.36 Å by using the HRTEM image in Figure 1a. The values agree with the distances of the SADP-marked dotted planes calculated from Figure 1b, as well as the XRD results shown in Figure S1. The inset of Figure 1a shows the fast Fourier transformed (FFT) pattern converted from the whole HRTEM image of Figure 1a. The result shows good accordance with that from the SADP in Figure 1b, which verifies good crystallinity of the multilayer GeS.

Figure 1c shows the atomic arrangement of orthorhombic GeS viewed along *c* (top), *b* (lower, left), and *a* (lower, right) crystal axes. Like the atomic configuration according to HRTEM as shown in Figure 1a, there are many diamond-shaped units in the *c* plane with an average Ge−S bond length of about 2.5 Å.[8] The larger bond length is about 2.8 Å (d_{110}) along the [110] direction of the layer. The monolayer, when viewed along *b* and *a* axes, exhibits totally different Ge−S bond connections. An armchair atomic chain extends along the *a* axis while a zigzag-type connection is constructed along the *b* axis for monolayer GeS. Because the formation of GeS arises from the bonding connection of the valence electrons Ge $4s^2 4p^2$ and S $3s^2 3p^4$, the armchair type and zigzag connections of the Ge−S along *a* and *b* may be the origin of structural and optical anisotropy of the GeS thin layer; for example, the armchair chain consists of atoms connected as (higher S)−(higher Ge)−(lower S)−(lower Ge)−(higher S), and so on, that along the *a* axis (see lower left of Figure 1c). The bond connections of the (higher Ge)−(lower S) or (lower Ge)−(higher S) bonds in the armchair chain may be dipolar as in Ge(+) → S(−), which presents dipole moments only vectored normal to the layer (*c*) plane with up and down directions. Transitions of up-and-down bond dipole moments (normal to the layer) in GeS should only be allowed with polarization along the *a* axis, but they may be forbidden with E||*b* polarization. We will show and discuss the optical results later.

The polarization-dependent μPL and *μ*Raman spectra of a multilayer GeS with thickness about 40 nm are shown in **Figure 2**a,b. The sample image and AFM results of the multilayer GeS flakes are shown in Figure 2c. The thickness of part B is about 40 nm and part A is a three-step stack of up to about 270 nm. Most of the GeS nanoflakes in Figure 2c reveal a longest crystal edge along the *b* axis, which is convenient to carry out polarization-dependent optical measurements of the GeS multilayer. Figure 2a shows the polarized μPL spectra of the GeS multilayer along E||*a* and E⊥*a* (E||*b*) polarizations for different thickness GeS of A and B in Figure 2c. The band-edge emission (BE, ca. 1.622 eV) was irradiated with an electric field along the *a* axis, while radiation is fully forbidden in the E||*b* polarized direction for both A and B portions. This work

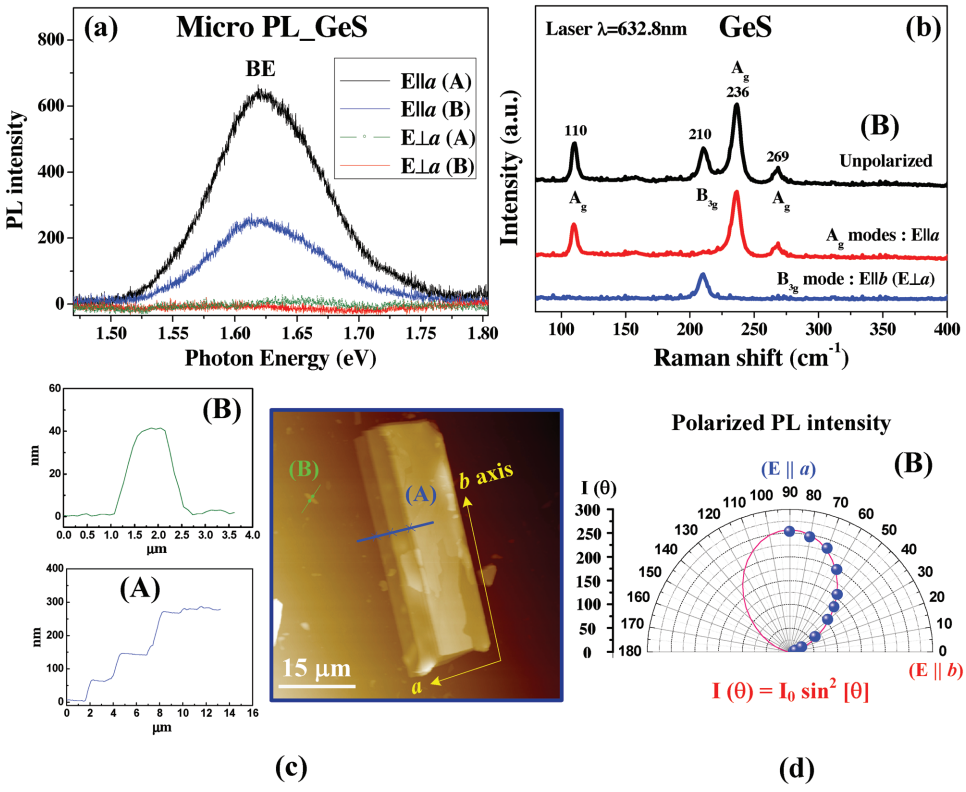

Figure 2. a) Polarized μPL spectra of multilayer GeS with thickness around 40 nm. The measurements were done with the linearly polarized light along and perpendicular to the *a* axis. The polarized μPL spectrum of a thicker GeS sample (270 nm) is also included for comparison. b) Polarized *μ*Raman spectra of GeS multilayer using red laser. c) Optical microscope image and AFM results of the GeS multilayer nanoflakes used for μPL and *μ*Raman measurements. B is about 40 nm and A is a three-step stack to about 270 nm. d) Angular dependence of the polarized PL intensity from E||*b* ($\theta = 0°$) to E||a ($\theta = 90°$) which derives from B [measured in (a)].

is unique in polarization-dependent PL emission for a thin multilayer GeS at 300 K. A Si-doped bulk GeS also revealed a similar radiation of E||a at 1.7 K.[21] This result can verify our room-temperature polarized μPL result of the thin multilayer GeS in Figure 2a. The selection rule of the BE-PL emission can be attributed to the transition dipole moment along the a or b axis of the multilayer GeS. The electronegativities of Ge and S are respectively 2.0 and 2.6, which results in an electronegativity difference of 0.6 and allows formation of polar covalent bonding in the GeS (i.e., electronegativity difference, 0 < polar covalent bond < 2). The bond polarity of Ge(+) → S(–) of the up-and-down bond dipole moments (normal to the layer) may mutually connected only along the armchair chain direction of a axis. Therefore, the polarization behavior of the optical transition along and perpendicular to the a axis may be clearly shown by GeS. In general, the dipole operator is $\boldsymbol{d} = q.\mathbf{r}$, where q is the charge and r is a vector in an axial direction. The dipole operator $\boldsymbol{d}$ can be a matrix element in space by axial directions and the transition probability of electron–hole pair recombination from initial state $|\psi_i>$ to final state $|\psi_f>$ can be:

$$<\psi_i|d|\psi_f> = \int \psi_i^* \; d\psi_f \mathrm{d}^3\mathrm{r} = q \cdot \int \psi_i(\mathrm{r})^* \cdot \mathbf{r} \cdot \psi_f(\mathrm{r}) \mathrm{d}^3\mathbf{r} \quad (1)$$

If the result of matrix element in spatial overlapping of the wavefunctions from $|\psi_i>$ to $|\psi_f>$ is zero, the transition is forbidden. This situation is similar to the BE–PL emission along the E||b polarization in Figure 2a. Existence of allowed and forbidden transitions in a semiconductor usually occurs with a valence-band maximum ($\boldsymbol{E}_V$) consisting of a **p** orbital with quantum number l (spatial correlated k selection rule). This result verifies that the $\boldsymbol{E}_V$ of GeS is mainly composed of S 3**p** states.[8,22] The transition dipole moments along the a and along b axes should considerably different in the layered GeS. However, more theoretical calculations of the bond structure need be carried out to verify this point.

The angular dependence of the polarized PL intensity $\boldsymbol{I}(\theta)$ of the multilayer GeS (B part) from $\theta = 0°$ (E||b) to $\theta = 90°$ (E||a) was also characterized by polarized μPL experiments. The solid circles in Figure 2d display the experimental results with polar co-ordination. The solid line is fitted to a dichroic relation of polarized light by using Malus law to the PL intensity:[18]

$$\boldsymbol{I}(\theta) = \boldsymbol{I}_0 \cdot \sin^2[\theta] \quad (2)$$

The experimental values match well with the fitted result using Eq. (2). The fitted value of $I_0 \approx 257$. The emission light of GeS is largely a [100]-polarized radiation along the a axis. Moreover, Figure 2a also shows the thicker multilayer GeS sample (black line, E||a from A ca. 270 nm), which possesses higher PL intensity than that of the thinner one (blue line, E||a from B ca. 40 nm) by three times. With decreasing thickness to monolayer, GeS becomes an indirect semiconductor,[8] which destroys the luminescence efficiency. This loss of luminescence may be one reason that decreasing thickness results in reduction of PL intensity of the GeS multilayer. The other reason is the band-edge emission (BE), which is largely caused by the up-and-down bond dipole moments (normal to the layer plane) having [100] polarized light. Greater stacking of the GeS layer (A part) will enhance the [100] polarized emission intensity of the up-and-down Ge—S bonds in the armchair chains. Furthermore, to identify in-plane structural anisotropy of the GeS multilayer on the c plane, polarized μRaman measurement with unpolarized, $c(a,a)\overline{c}$, and $c(a,b)\overline{c}$ polarizations were carried out. The experimental results are given in Figure 2b. Four vibration peaks at 110, 210, 236, and 269 cm^{-1} (corresponding to A_g and B_{3g} symmetric modes) can be clearly detected by the unpolarized spectrum of the multilayer GeS (B part). These observed modes are similar to previous Raman results for bulk GeS.[23,24] The A_g and B_{3g} modes are in-plane stretch and vibrated frequencies of the GeS layer with shaken directions along armchair (a) and zigzag (b) axis. The relative Ge—S shear motions of A_g and B_{3g} modes can be observed along different orientations by polarized μRaman measurement. Figure 2b clearly shows that the armchair-related modes A_g (110, 236, and 269 cm^{-1}) can be detected at E||a polarization [$c(a,a)\overline{c}$] while the B_{3g} peak (210 cm^{-1}) is only allowed in the E||b orientation [$c(a,b)\overline{c}$]. The result clearly verifies the in-plane structural anisotropy of the a–b axes of multilayer GeS.

To further study the band-edge emission of multilayer GeS, low-temperature μPL measurements were implemented. **Figure 3**a shows the unpolarized μPL spectrum of the multilayer GeS (B part) between 1.25 and 1.8 eV at 10 K. There are two main peaks, denoted as DAP and FX and observed at ca. 1.553 and 1.732 eV, for the multilayer GeS. The DAP feature is assigned to be donor–acceptor–pair emission of the multilayer GeS, and is evident by power-dependent μPL measurements at 10 K in Figure S2(a), see Supporting Information. The energy position of the DAP emission will increase with the incident power of the laser. The low-temperature FX feature in Figure 3a is free-exciton emission of the multilayer GeS that corresponds to that of BE as detected in Figure 2a at 300 K (i.e., the energy is 1.622 eV at 300 K and 1.732 eV at 10 K). This experiment also reveals the transition selection rule of E||a (allowed) and E⊥a (forbidden), shown in Figure 3b at 10 K. The polarization dependence verified that the 1.732 eV emission peak (FX) is coming from the band-edge free exciton of multilayer GeS. Figure 3c also shows a temperature-energy shift of the FX peak. As the temperature increases, the energy value of the FX emission decreases, like general semiconductor behavior. The ionization temperature of FX is about 77 K ($kT \approx 6.6$ meV) and the value matches well with the binding energy of bulk GeS.[12] When $T > 77$ K, the FX is ionized and the band-to-band emission BE will eventually dominate the main photoluminescence intensity up to 300 K. Besides, as shown in Figure 3a, the signal due to DAP is stronger than that of the FX emission; this indicates strong imperfection (impurity and defect levels) localization effect at low temperature. With increased temperature, the ionization effect (delocalization) will reduce the PL intensity of the DAP, such as that shown in Figure S2(b).

To characterize the anisotropic band-edge property of the multilayer GeS, PTR measurement of a GeS multilayer nanoflake was also implemented. An LGM system with an object lens (×50) was used to guide the incident and reflected white lights of the multilayer sample under thermal modulation (see **Figure 4**c). A pair of dichroic sheet polarizers facilitated the PTR measurements with E||a and E||b polarizations. Figures 4a,b are the PTR spectra of the multilayer GeS at 300 and 30 K, respectively. The microscope image of the multilayer sample is shown in Figure 4c, and the AFM result is also included for comparison. The thickness of the sample was about 60 nm and the a–b

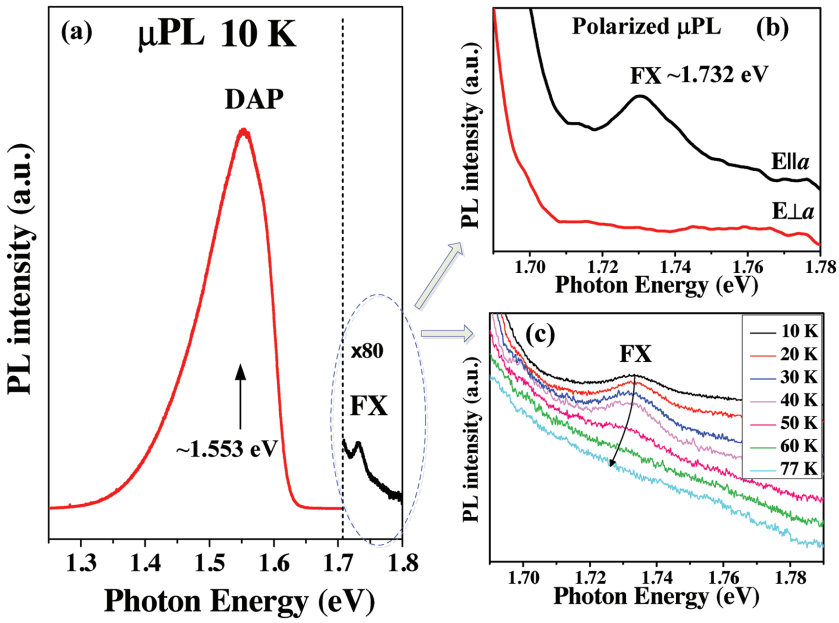

Figure 3. a) μPL spectrum of the multilayer GeS near band edge at 10 K. b) Polarized PL spectra of E||*a* and E⊥*a* of the free-exciton emission at 10 K. c) Temperature dependence of the free-exciton emission FX of the multilayer GeS from 10 to 77 K.

axial directions are clearly indicated in the microscope image of Figure 4c. TR is a very powerful tool for evaluation of optical transitions near band edges.[25] The derivative spectral line shape of the transition feature enhances the ability to determine the exact energy location of the direct transition in semiconductors. Displayed in Figure 4a,b are the PTR spectra of multilayer GeS at 300 and 30 K, together with the corresponding μPL spectra of BE and FX emissions for comparison. The dashed lines in Figure 4a,b are the experimental PTR data, and solid curves are the least-square fits to a first derivative Lorentzian line-shape function appropriate for the band-edge transition feature expressed as:[26]

$$\frac{\Delta R}{R} = \mathrm{Re}\left[Ae^{j\varphi}(E - E_g - j\Gamma)^{-2}\right] \quad (3)$$

where A and φ are the amplitude and phase of the line shape, and E_g and Γ are energy and broadening parameters of the excitonic transition in the multilayer GeS. The fits yield transition energy values of E_A = 1.622 and E_B = 1.732 eV at 300 K, and E_A = 1.730 and E_B = 1.843 eV at 30 K. The energy positions of the E_A transition approximately match well with the BE and FX emission peaks at room and low temperatures. The E_A transition is present only along the E||*a* polarization while the E_B transition appears only in the E||*b* polarized spectra. In-plane optical anisotropy of the multilayer GeS is clearly

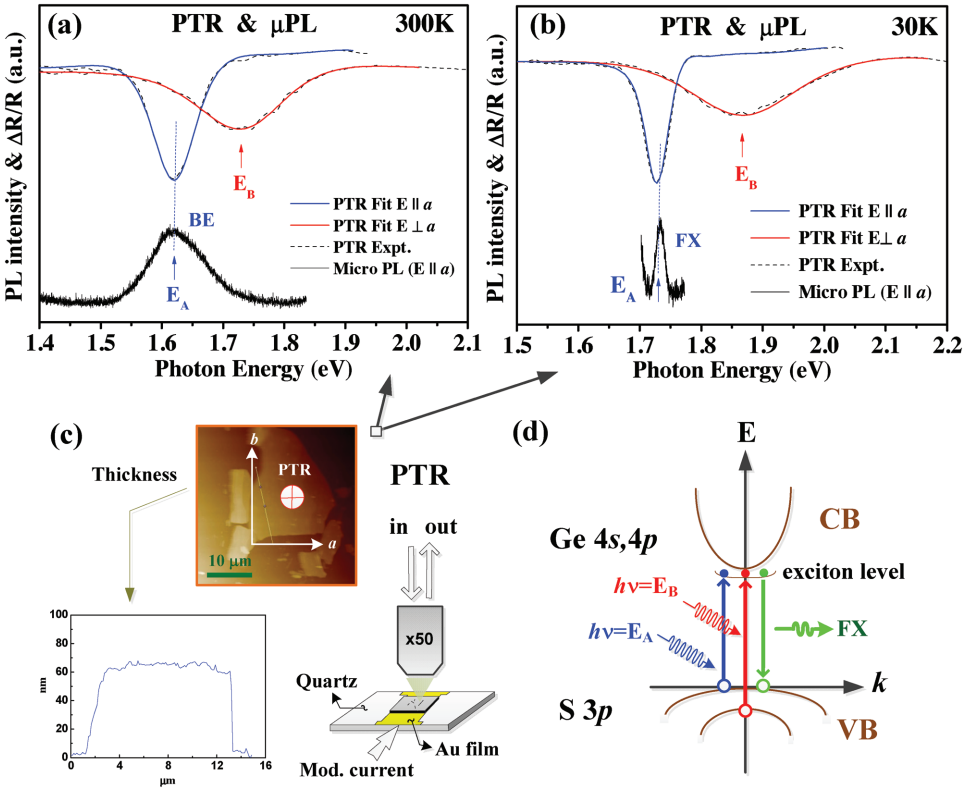

Figure 4. The PTR and μPL spectra of the multilayer GeS near band edge at a) 300 and b) 30 K. c) The optical-microscope image and AFM result of the multilayer GeS sample. The measurement configuration of the white-light microscope guiding system of TR is also included for comparison. d) The probable band-edge scheme of multilayer GeS at low temperature proposed based on PTR and μPL measurements.

shown; it is similar to the polarized PL result in Figure 2a. The main difference between the transition mechanisms in PL and TR measurements is that the photon emission of PL is a recombination process from laser-excited electron–hole pairs in semiconductors. The laser-excited electron–hole pairs should be hot carriers, and they may relax (heat and phonon) down to the lowest energy states of conduction band (CB) and valence band (VB), like the band edge, to make a major recombination and hence emitting a main PL peak. Therefore, the main PL peak usually occurs at the lowest energy states of BE (E_A), as for the experimental result shown in Figure 4a. However, for TR measurement, the direct interband transitions from VB to CB above band edge can be fully detected owing to the high transition probability from occupied VB to empty CB states. This probability is why the E_B transition can be clearly detected by TR but is very weak in the PL spectra of Figures 2a and 4a. Furthermore, to verify the direct band-gap of GeS, transmittance measurement was also implemented at 300 K. The transmittance spectrum is shown in Figure S3 in the Supporting Information. The absorption edge of transmittance spectrum ranges from ca. 1.55 to 1.72 eV, matching well with the BE emission and E_A transition that detected in Figure 4a. The spectrum shows direct semiconductor behavior of GeS. Figure 4d depicts the possible band-edge scheme of multilayer GeS based on the low-temperature optical measurements and with reference to previous band-structure calculations.[10] The conduction band CB is mainly composed of Ge 4s and 4p antibonding states and the VB maximum is dominated by S 3p bonding states. The exciton level near CB has a binding energy of ca. 6.6 meV. The FX emission originates from the CB exciton level to the VB top at low temperature. The exciton level is ionized at 60–70 K. The E_A transition originates from VB top to the CB transition while the E_B feature (by PTR) may come from valence-band splitting using optical polarization along the *b* axis. The dichroic behavior and in-plane optical anisotropy of the thin multilayer GeS could render it a potential material for fabrication of polarized-light emitters and polarization-sensitive photodetectors.

In conclusion, linearly polarized-light emission of *c*-plane multilayer GeS (t ≈ 40 nm) with an electric field along the *a* axis was demonstrated by use of polarized μPL measurement at 300 K. The band-edge emission light at 1.622 eV follows a dichroic Malus-law relation with the fully allowed radiation along *a* polarization and the completely forbidden luminescence along the E||*b* polarized condition. The structural anisotropy of the *c* plane GeS multilayer along the *a* and *b* axes was also identified by polarized μRaman measurements with $c(a,a)\overline{c}$ and $c(a,b)\overline{c}$ polarizations. The A_g related modes only present along the E||*a* polarized condition while the B_{3g} mode appears only along the *b* axis polarization. In PTR measurements, the multilayer GeS (t ≈ 60 nm) shows band-edge transition E_A present at E||*a* while transition E_B occurred at E||*b* polarized condition. The energy position of E_A matches well with the band-edge emission at 1.622 eV. The result verifies the direct semiconductor behavior of the multilayer GeS. In-plane optical anisotropy of the multilayer GeS is completely demonstrated by optical radiation and band-edge transition by μPL and PTR experiments. All the experimental results validate the multilayer GeS as being a potential 2D material suitable for application in polarization-sensitive light emitters and absorbers.

Supporting Information

Supporting Information is available from the Wiley Online Library or from the author.

Acknowledgments

This work was sponsored financially by the Ministry of Science and Technology, Taiwan under grant nr. MOST 104-2112-M-011-002-MY3. We are thankful to Prof. S. Y. Chen in the Materials Science & Engineering department, NTUST, for technical assistance.

Received: October 5, 2016
Published online: November 25, 2016

[1] D. Ovchinnikov, F. Gargiulo, A. Allain, D. J. Pasquier, D. Dumcenco, C.-H. Ho, O. V. Yazyev, A. Kis, *Nat. Commun.* **2016**, *7*, 12391.
[2] B. Radisavljevic, A. Radenovic, J. Brivio, V. Giacometti, A. Kis, *Nat. Nanotechnol.* **2011**, *6*, 147.
[3] C. H. Ho, *2D Mater.* **2016**, *3*, 025019.
[4] R. K. Ulaganathan, Y. Y. Lu, C. J. Kuo, S. R. Tamalampudi, R. Sankar, K. M. Boopathi, A. Anand, K. Yadav, R. J. Mathew, C. R. Liu, F. C. Chou, Y. T. Chen, *Nanoscale* **2016**, *8*, 2284.
[5] K. F. Mak, C. Lee, J. Hone, J. Shan, T. F. Heinz, *Phys. Rev. Lett.* **2010**, *105*, 136805.
[6] C. C. Wu, C. H. Ho, W. T. Shen, Z. H. Cheng, Y. S. Huang, K. K. Tiong, *Mater. Chem. Phys.* **2004**, *88*, 313.
[7] W. Feng, W. Zheng, W. Cao, P. Hu, *Adv. Mater.* **2014**, *26*, 6587.
[8] F. Li, X. Liu, Y. Wang, Y. Li, *J. Mater. Chem. C* **2016**, *4*, 2155.
[9] L. Makinistian, E. A. Albanesi, *Phys. Rev. B* **2006**, *74*, 045206.
[10] T. Grandke, L. Levy, *Phys. Rev. B* **1977**, *16*, 832.
[11] B. D. Malone, E. Kaxiras, *Phys. Rev. B* **2013**, *87*, 245312.
[12] J. D. Wiley, A. Breitschwerdt, E. Schönherr, *Solid State Commun.* **1975**, *17*, 355.
[13] G. Valiukonis, D. A. Guseinova, G. Krivaite, A. Šileika, *Phys. Status Solidi B* **1986**, *125*, 299.
[14] Y. J. Cho, H. S. Im, Y. Myung, C. H. Kim, H. S. Kim, S. H. Back, Y. R. Lim, C. S. Jung, D. M. Jang, J. Park, E. H. Cha, S. H. Choo, M. S. Song, W. Cho II, *Chem. Commun.* **2013**, *49*, 4661.
[15] F. Lukeš, E. Schmidt, A. Lacina, *Solid State Commun.* **1981**, *39*, 921.
[16] D. D. Vaughn II, R. J. Patel, M. A. Hickner, R. E. Schaak, *J. Am. Chem. Soc.* **2010**, *132*, 15170.
[17] C. Li, L. Huang, G. P. Snigdha, Y. Yu, L. Cao, *ACS Nano* **2012**, *6*, 8868.
[18] E. Hecht, in *Optis*, 4th ed, Addison Wesley, San Francisco, CA **2002**, p. 333.
[19] C. H. Ho, *J. Mater. Chem.* **2011**, *21*, 10518.
[20] C. H. Ho, H. W. Lee, Z. H. Cheng, *Rev. Sci. Instrum.* **2004**, *75*, 1098.
[21] W. Senske, R. A. Street, A. Nowitzki, P. J. Weisner, *J. Lumin.* **1978**, *16*, 343.
[22] R. B. Shalvoy, G. B. Fisher, P. J. Stiles, *Phys. Rev. B* **1977**, *15*, 2021.
[23] H. C. Hsueh, M. C. Warren, H. Vass, G. J. Ackland, S. J. Clark, J. Crain, *Phys. Rev. B* **1995**, *53*, 14806.
[24] J. D. Wieley, W. J. Buckel, R. L. Schmidt, *Phys. Rev. B* **1976**, *13*, 2489.
[25] C. H. Ho, C. H. Lin, Y. P. Wang, Y. C. Chen, S. H. Chen, Y. S. Huang, *ACS Appl. Mater. Interfaces* **2013**, *5*, 2269.
[26] D. E. Aspnes, in *Optical properties of solids, Handbook on Semiconductors*, Vol. *2*, (Ed.: M. Balkanski), Amsterdam, The Netherlands **1980**, p. 109.

ADVANCED OPTICAL MATERIALS

Supporting Information

for *Adv. Optical Mater.*, DOI: 10.1002/adom.201600814

Polarized Band-Edge Emission and Dichroic Optical Behavior in Thin Multilayer GeS

Ching-Hwa Ho and Jia-Xuan Li*

Supplementary Information

Polarized band-edge emission and dichroic optical behavior in thin multilayer GeS

Ching-Hwa Ho,[*1,2] Jia-Xuan Li[1]

[1] *Graduate Institute of Applied Science and Technology, National Taiwan University of Science and Technology, Taipei 106, Taiwan*

[2] *Graduate Institute of Electro-Optical Engineering and Department of Electronic and Computer Engineering, National Taiwan University of Science and Technology, Taipei 106, Taiwan*

[*]E-mail: chho@mail.ntust.edu.tw

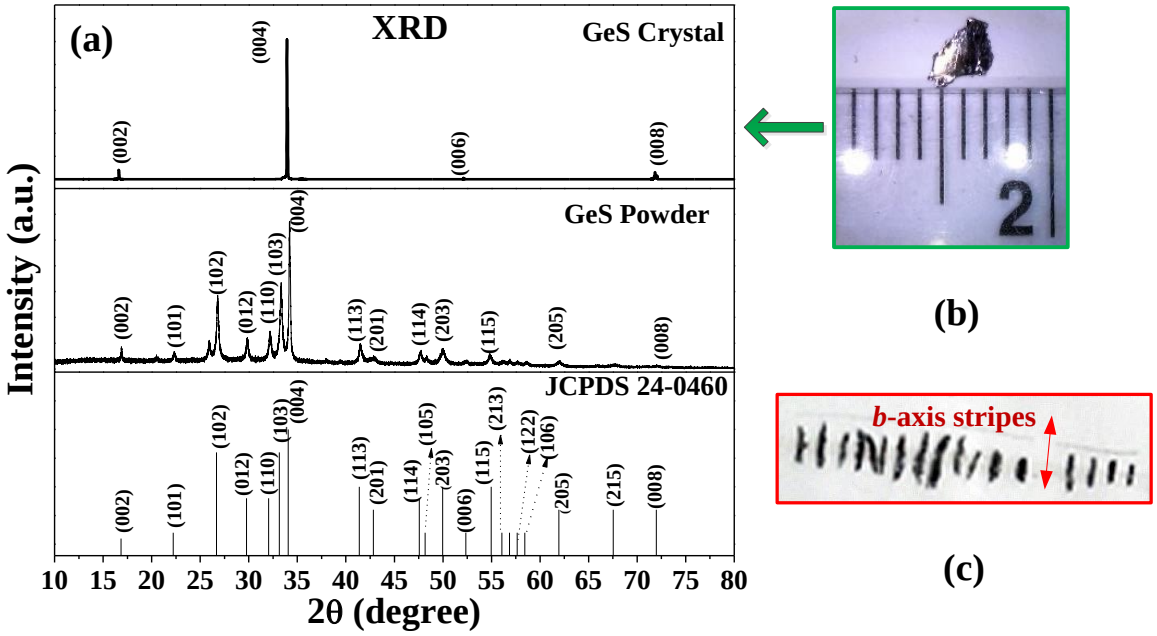

Figure S1. (a) X-ray diffraction (XRD) pattern of single layered crystal (top), powder GeS (middle), and JCPDS data (lower) for the germanium monosulfide. (b) The as-grown GeS layer crystal used for single-crystal XRD measurement with a larger area size. (c) The easily forming shapes of GeS layer crystal with a longest edge along *b* axis. They are usually *b*-axis stripes with different thicknesses.

Figure S1 respectively shows the XRD patterns of the as-grown GeS single crystal, small GeS crystal ground into powder, and JCPDS card data 24-0460 [27] for the comparison of crystal structure of germanium monosuifide. The single-crystal XRD data are derived from the as-grown crystal shown in Figure S1(b). The XRD result only shows the *c*-plane higher order peaks and reveals layer-type structure of the GeS. The powder XRD data match well with the JCPDS data in Fig. S1(a) identifies orthorhombic crystal phase of the as-grown crystals. The lattice constant of the crystals was determined to be a=4.36 Å , b=3.67 Å , and c=10.53 Å . The outline shapes of the GeS crystals are usually shown in a longest crystal edge along *b* axis as observed in Figure S1(c).

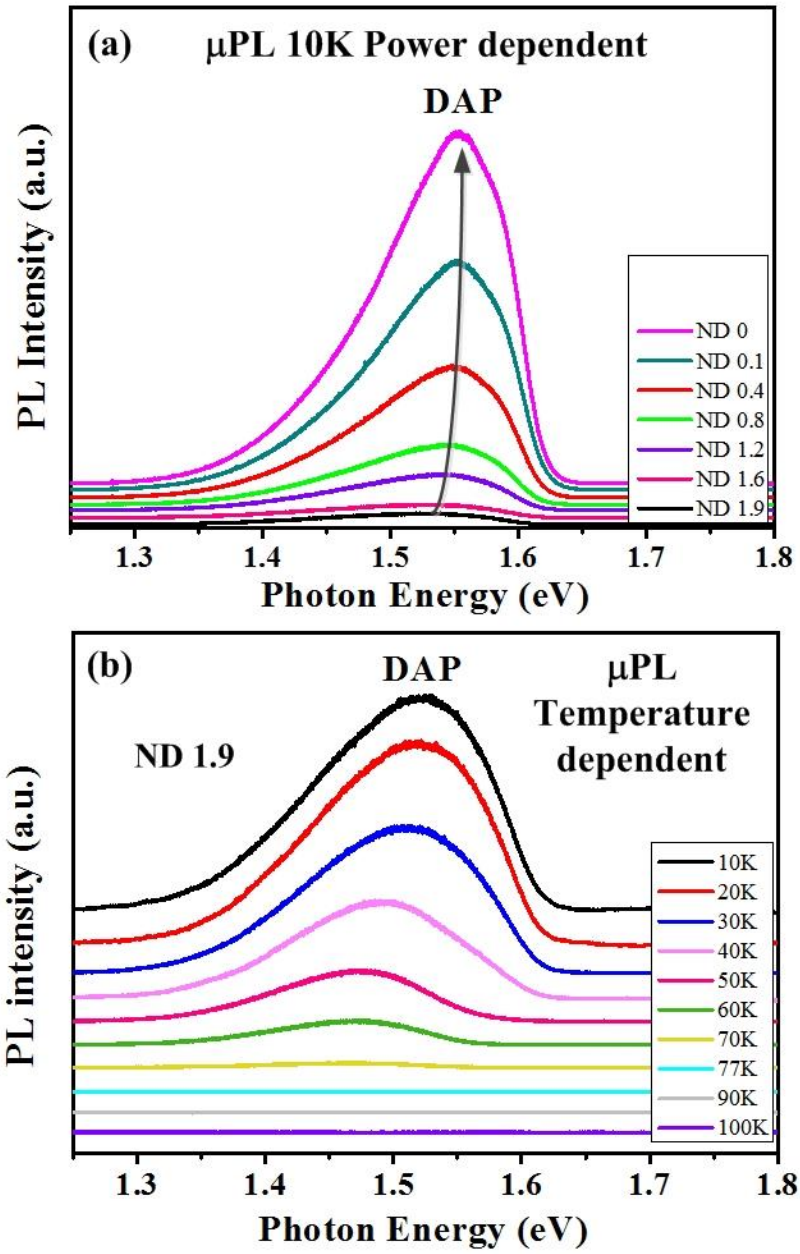

Figure S2. (a) Power-dependent μPL spectra of the GeS thin multilayer at 10 K for the donor-acceptor-pair (DAP) emission with the laser incident powers from full power (ND 0) to $\times 10^{-1.9}$ (ND 1.9). The laser wavelength is 633 nm. Full output power is 21 mW. (b) The temperature dependence of DAP emission with a lower power excitation of ND 1.9.

Figure S2(a) shows the power-dependent PL spectra of the DAP emission of the multilayer GeS as displayed in Figure 3(a). As the incident power of laser is increased,

the energy position of the DAP peak increases from ~1.523 eV (ND 1.9) to ~1.553 eV (ND 0). The energy of DAP emission is closely related to the DAP's distance *r* in Coulombic energy expressed as: $E_{DAP} = E_g - E_D - E_A + e^2/(4\pi\varepsilon r)$, where E_D and E_A are the binding energies of donor and acceptor, e is the electron charge, and ε is the permittivity of the material. With the increase in excitation power, the photoexcited DAPs become high density; then, the average distance *r* shortened to increase photon energy. The increase of DAP energy with laser power in Figure S2(a) indicates it may come from the donor-acceptor-pair emission such as the direct semiconductor In_2O_3 [28]. Figure S2(b) shows temperature-dependent μPL spectra of the DAP emission from 10 to 100 K (i.e. with ND 1.9 laser excitation). When the temperature increased, the intensity of DAP weakened, and which shifted to lower energy. When T >77 K, the donor-acceptor-pair ionized to decrease the DAP emission. It means that the ionization temperature of the shallow-level DAP emission is around 77 K.

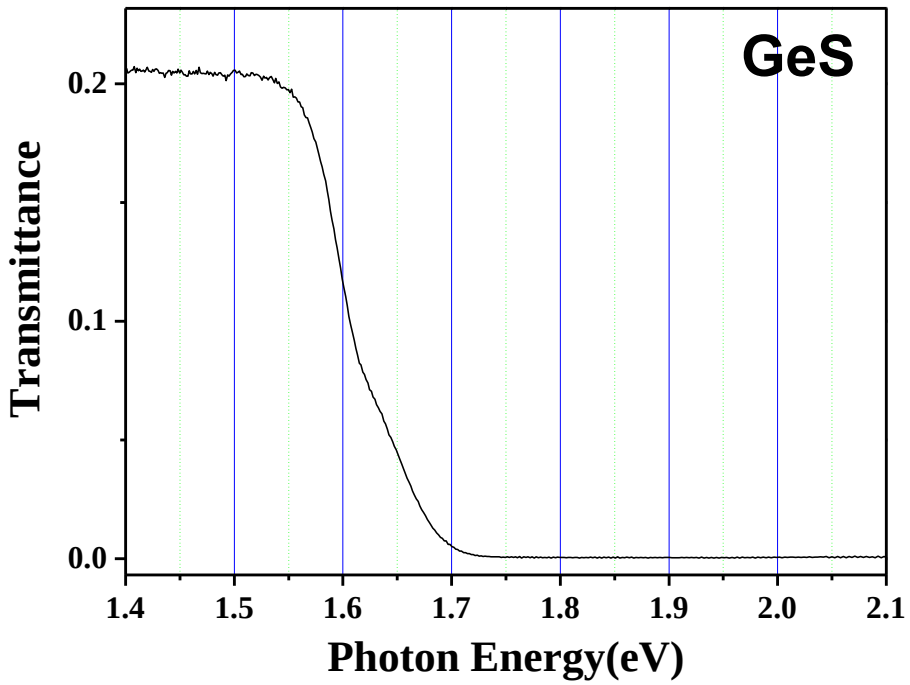

Figure S3. Transmittance spectrum of a bulk GeS layer crystal (50-μm thick) near band edge from 1.4 to 2.1 eV at 300 K. The energy portion of absorption edge (1.55-1.72 eV) shows matching well with the PL peak and the TR transition feature of E_A displayed in Fig. 4(a). The result indicates direct-band-edge character of the GeS layered crystal.

As shown in Fig. S3 is the transmittance spectrum of a bulk GeS layered crystal with thickness of ~50 μm. The transmittance value is about 0.21 below 1.5 eV. It is clearly the absorption edge ranges from ~1.55 eV to ~1.72 eV, matching well with the PL and TR results of the E_A transition in Figure 4(a) for GeS. The experimental result identifies direct semiconductor behavior of the GeS.

Supplementary Information References:

27. E.-i Shimazaki, T. Wada, *Bull. Chem. Soc. Jpn.* **1956**, *29*, 294.
28. C. H. Ho, C. H. Chan, L. C. Tien, Y. S. Huang, *J. Phys. Chem. C* **2011**, *115*, 25088.